

Fig. 5. Thresholds ($|c| \equiv \tau\Sigma\gamma/|\beta|\zeta$ vs. E) of the pulse stability. The different colors correspond to $b \equiv \gamma/\zeta = 0.001$ (black), 0.1 (red), and 10 (blue); $\mu = 0.008$. Analytical thresholds from [20] correspond to the curves (the CDS are stable in the direction of the arrows marked in regular type). Analytical thresholds from the variational model correspond to the symbols (the CDS are stable in the direction of the arrows marked in italics).

The appearance of the additional degree of freedom (b -parameter) calls for comment. The decrease of ζ (i.e. the b -growth due to suppression of the SAM with simultaneous decrease of the normalized E and the c -growth) almost does not affect the DS stability if other parameters (including the dimensional energy E) are fixed and $|c|/\mu < 1$. This results from the opposite directions of shifts of the dimensionless E (to the left) and the stability threshold (to the right) with simultaneous compensating c -growth ($\propto 1/\zeta$). It should be noted that the DS becomes unstable if $|c|/\mu > 1$. If this occurs, additional growth of $|\beta|$ is required. Physically, the ζ -decrease for a fixed SESAM can be provided at the expense of a larger mode size on it.

The decrease of γ (the b -decrease due to SPM suppression) enhances the DS stability if other parameters (including the dimensional energy E) are fixed. This effect results from a slower dependence of $|c|$ on E in relation to that in the ADR. Physically, it can be realized by means of cavity purification for a thin-disk oscillator or by using a large-area fiber for an ANDi fiber laser. It should be noted here that such stability enhancement is not so substantial in relation to a Kerr-lens mode-locked oscillator obeying the cubic-quintic CNGLE [18, 20], because there is no an asymptotic $c = const$ for $E \rightarrow \infty$ for the generalized CNGLE (Figs. 3, 5 cf. Fig. 6 in [18]).

From the point of view of the master diagrams in Fig. 5, the almost ideal energy scalability corresponds to an ANDi fiber laser (if the spectral dissipation is defined by a spectral filter). Simple length scaling would result in proportional scaling of γ and $|\beta|$. Hence, the $|c|$ -parameter remains constant. Simultaneously, the shift of the stability border to the right (due to b -growth) would provide the conditions for almost proportional energy growth (if $|c| \ll 1$).

It should be noted that the dependence of the threshold curves on b (i.e. three-dimensionality of the master diagram) in the model under consideration is in completely agreement with the dependence of such a threshold on only the two parameters c and E in [15, 18] for $|c| \ll 1$. Figure 5 suggests that the master diagram would become two-dimensional for $|c| \ll 1$ if the energy is normalized to the value $\propto \zeta^2/\gamma\sqrt{\tau}$. This means that the curves in Fig. 5 would merge (and the curves represented by symbols would merge for $|c| \ll 1$) if one transits from E to E/b

for fixed μ (see Fig. 6). Thus, this normalization in combination with the definition of c can be considered as the scaling law for the NDR in the $|c| \ll 1$ limit.

Physically, the re-scaled master diagram can be divided into three main regions (Fig. 6): i) $b \ll 1$ corresponds to a thin-disk solid-state oscillator (black curve and crosses; see Table 2 and black circle); ii) $b > 1$ corresponds to ANDi fiber oscillator (red curve; see Table III in [20] and red squares in Fig. 6); and iii) $b < 1$ corresponds to a broad-band solid-state oscillator (blue curve; see Table IV in [20] and blue triangle). One can see that the scaling rules under consideration are valid within an extremely broad range of parameters covering both solid-state (bulk and thin-disk) and fiber oscillators operating in the NDR. It should be noted that strong pulse breathing during its evolution in a fiber oscillator can deform the master diagram, and this effect calls for additional study.

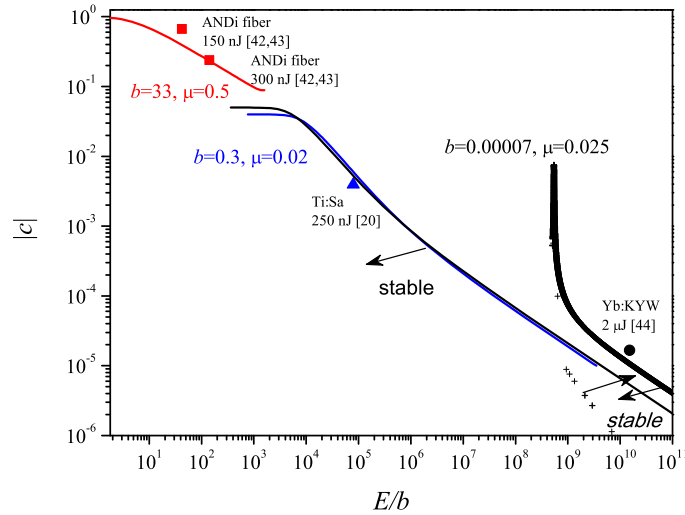


Fig. 6. Thresholds ($|c| \equiv \tau\Sigma\gamma/|\beta|\zeta$ for the solid-state oscillators and $|c| \equiv \tau\gamma/|\beta|\zeta$ for the fiber ones vs. E/b) of the pulse stability. The different colors correspond to $b \equiv \gamma/\zeta = 33$ and $\mu = 0.5$ (red), $b = 0.3$ and $\mu = 0.02$ (blue), $b = 7 \times 10^{-5}$ and $\mu = 0.025$ (black). Analytical thresholds from [20] correspond to the curves (the CDS is stable in the direction of the arrow marked in regular type). Analytical threshold from the variational model is shown by crosses (the CDS is stable in the direction of the arrows marked in italics). Symbols demonstrate the operational points in the vicinity of the stability threshold for the different oscillators (corresponding references and output energies are given).

5. Conclusion

The analytical theory of dissipative soliton (DS) energy scalability is presented. The theory is based on the variational approach to generalized CNGLE modeling of an oscillator mode-locked by a perfectly saturable absorber, e.g. a SESAM. The solutions presented cover two physically important cases: oscillators operating in the anomalous dispersion regime (ADR) and the normal dispersion regime (NDR).

It is found that the ADR is characterized by a two-dimensional master diagram connecting the DS stability with the relative contribution of dissipative and nondissipative effects for a given DS energy. Such a relative contribution is described by the sole parameter $c \equiv \tau\Sigma\gamma/|\beta|\zeta$ (or $c \equiv \tau\gamma/|\beta|\zeta$ when the spectral dissipation is defined by a filter), which can easily be expressed through the values of the oscillator dispersion (β), self-phase modulation (γ), squared inverse

gain bandwidth (τ), self-amplitude modulation (ζ), and net loss (Σ). Two different sectors of the ADR master diagram are found: one corresponding to a scaling pulse width and the other to an almost constant pulse width. For the latter, the c -parameter depends on the energy almost linearly. This means that the dispersion has to be increased, and/or the self-phase modulation has to be decreased, and/or the spectral filter bandwidth has to become broader with the growing energy. The approximated scaling rule for a dimensional energy in the constant pulse width sector can be formulated as

$$cE\zeta/\sqrt{\tau\Sigma} \approx \ell, \quad (13)$$

where ℓ grows almost linearly with the modulation depth parameter μ , and Σ appears only if the spectral dissipation is dominated by a gain-band (otherwise $\Sigma=1$).

The main results in the AND are verified by numerical simulations for thin-disk high-energy Yb:YAG oscillators. Moreover, it is demonstrated that a broad range of oscillators (both solid-state and fiber ones) fits to the model proposed.

The NDR providing CDS generation is characterized by a three-dimensional master diagram in the general case. The CDS is stabilized by substantially reduced (approximately tenfold) dispersion $|\beta|$ in relation to that in the ADR. The already proposed approximated model [20] is in perfect agreement with the numerical simulation for thin-disk Yb:YAG oscillators. Simultaneously, comparison between the model presented and that of Ref. [20] demonstrates that the latter breaks when $|c|/\mu \rightarrow 1$. The approximated scaling rule for $|c| \ll 1$, where the master diagram becomes two-dimensional, can be formulated as

$$E\zeta^2 c^2 / \gamma \sqrt{\tau\Sigma} \approx \Upsilon, \quad (14)$$

where Υ is the growing function of μ slowly varying with c . This rule covers all types of oscillators. For solid-state oscillators, this scaling rule suggests a substantial reduction of dispersion and the need for SPM suppression in the NDR. For ANDi fiber oscillators, the scaling rule is almost perfect: fiber length scaling provides almost linear scaling of the CDS energy.

The main results in the NDR are verified numerically for the thin-disk Yb:YAG oscillators as well. It is demonstrated that the analytical model fits the real-world oscillators with parameters covering an extremely wide range.

Acknowledgements

This work was supported by the Austrian Fonds zur Förderung der wissenschaftlichen Forschung (FWF project P20293) and the Munich Centre for Advanced Photonics (MAP). The authors thank O. Pronin and R.Graf for valuable and stimulating discussions as well as for providing the simulation parameters for the Yb:YAG oscillators.